

# TiO<sub>2</sub> Hollow Spheres Composed of Highly Crystalline Nanocrystals Exhibit Superior Lithium Storage Properties\*\*

Genqiang Zhang, Hao Bin Wu, Taeseup Song, Ungyu Paik, and Xiong Wen (David) Lou\*

**Abstract:** While the synthesis of TiO<sub>2</sub> hollow structures is well-established, in most cases it is particularly difficult to control the crystallization of TiO<sub>2</sub> in solution or by calcination. As a result, TiO<sub>2</sub> hollow structures do not really exhibit enhanced lithium storage properties. Herein, we report a simple and cost-effective template-assisted method to synthesize anatase TiO<sub>2</sub> hollow spheres composed of highly crystalline nanocrystals, in which carbonaceous (C) spheres are chosen as the removable template. The release of gaseous species from the combustion of C spheres may inhibit the growth of TiO<sub>2</sub> crystallites so that instead small TiO<sub>2</sub> nanocrystals are generated. The small size and high crystallinity of primary TiO<sub>2</sub> nanoparticles and the high structural integrity of the hollow spheres gives rise to significant improvements in the cycling stability and rate performance of the TiO<sub>2</sub> hollow spheres.

Hollow structures with low density, high surface area, and shell permeability have attracted increasing research interest because of their intriguing properties and widespread applications in various fields, including catalysis, drug delivery, sensors, energy storage, and others.<sup>[1–8]</sup> Researchers have developed various strategies to controllably synthesize different hollow structures for many materials.<sup>[2,9–16]</sup> Among these techniques, the hard-templating method, using polymers, silica, and other colloid particles as removable templates, has been considered to be one of the most versatile and straightforward strategies towards hollow spheres.<sup>[1,2,17,18]</sup> Hollow spheres of various materials, such as metals, metal oxides, and metal sulfides, have been prepared to date using hard-templating methods. For example, carbon-coated SnO<sub>2</sub> hollow spheres have been prepared through a designed multistep synthesis using silica spheres as the template.<sup>[19]</sup>

Despite many successes, some challenging issues remain in conventional hard-templating methods: a) prefunctionalization of the template surface or precise control of the deposition process is usually necessary to obtain uniform coating, b) the process is tedious because of the need to remove templates such as silica spheres, and c) partial collapse of the hollow structures commonly occurs after template removal. As a result, the facile synthesis of high-quality TiO<sub>2</sub> hollow spheres composed of highly crystalline nanocrystals is seldom reported, despite the fact that numerous TiO<sub>2</sub> hollow nanostructures have been reported by different templating or template-free methods. It is thus highly desirable and technologically important to develop simple and scalable strategies for the synthesis of high-quality TiO<sub>2</sub> hollow spheres.

The use of novel electrode materials is one of the central tasks in building the next generation of lithium-ion batteries (LIBs) with high power and energy densities for upcoming large-scale applications.<sup>[20–25]</sup> Anatase TiO<sub>2</sub> has been long studied as a promising anode material for LIBs because of its unique features, including low cost, environmental benignity, improved safety, and stability.<sup>[26–30]</sup> However, the low ionic and electrical conductivity which will cause limited capacity and poor cycling performance have seriously hindered its practical electrochemical performance.<sup>[31–33]</sup> It has been demonstrated that nanosized TiO<sub>2</sub> particles could effectively improve the Li<sup>+</sup> ion diffusion.<sup>[29,30]</sup> Unfortunately, severe aggregation of nanoparticles during the charge–discharge process imposes another challenge in practical applications. Recently, it has been proposed that TiO<sub>2</sub> hollow structures consisting of nanosized building blocks could partly overcome this problem while retaining high electrochemical activity.<sup>[28,31,32,34]</sup> However, most of the reported TiO<sub>2</sub> hollow structures exhibit less satisfactory long-term cycling stability, which is perhaps as a result of the low crystallinity and relatively large size of nanocrystallites and the poor structural stability of the hollow structures.

Herein, we report a simple and cost-effective template-assisted method to synthesize TiO<sub>2</sub> hollow spheres composed of highly crystalline nanocrystals. Carbonaceous (C) spheres are chosen as the removable template in view of several merits. C spheres can be readily obtained in large quantity from soluble carbohydrates such as glucose through a low-cost and environmentally friendly hydrothermal method. Importantly, the as-prepared C spheres possess rich hydrophilic functional groups, which are essential for their dispersion in solvents and the subsequent uniform deposition amorphous TiO<sub>2</sub> layer. Additionally, C spheres can be easily removed during calcination in air, which produces a highly crystalline TiO<sub>2</sub> product. It is possible that the release of

[\*] Dr. G. Q. Zhang, Prof. X. W. Lou  
TUM CREATE, 1 CREATE Way, #10-02 CREATE Tower  
Singapore 138602 (Singapore)

Dr. G. Q. Zhang, H. B. Wu, Prof. X. W. Lou  
School of Chemical and Biomedical Engineering  
Nanyang Technological University  
62 Nanyang Drive, Singapore 637459 (Singapore)  
E-mail: xwlou@ntu.edu.sg  
davidlou88@gmail.com

Homepage: <http://www.ntu.edu.sg/home/xwlou>

Dr. T. Song, Prof. U. Paik  
WCU Department of Energy Engineering, Hanyang University  
Seoul 133-791 (Korea)

[\*\*] This work was financially supported by the Singapore National Research Foundation under its Campus for Research Excellence and Technological Enterprise (CREATE) program.

Supporting information for this article is available on the WWW under <http://dx.doi.org/10.1002/anie.201406476>.



**Figure 1.** Illustration of the formation of  $\text{TiO}_2$  hollow spheres using carbon spheres as templates: a) amorphous  $\text{TiO}_2$  coating (blue) to form the  $\text{C@TiO}_2$  core/shell structure; b) thermal annealing treatment to form polycrystalline  $\text{TiO}_2$  hollow spheres (yellow).

gaseous species from combustion of C spheres inhibits the growth of  $\text{TiO}_2$  crystallites so that instead small  $\text{TiO}_2$  nanocrystals are generated. Together with a proper deposition method, high-quality  $\text{TiO}_2$  hollow spheres with a polycrystalline shell and excellent robustness are successfully prepared. The small size and high crystallinity of primary  $\text{TiO}_2$  nanoparticles and the high structural integrity of the hollow spheres gives rise to significant improvements in the cycling stability and rate performance of the  $\text{TiO}_2$  hollow spheres.

The synthesis of  $\text{TiO}_2$  hollow spheres is simple and straightforward, as illustrated in Figure 1. The C spheres obtained by a hydrothermal method<sup>[35]</sup> were well dispersed into anhydrous ethanol through sonication, followed by the addition of titanium tetrabutoxide (TTB) as the Ti precursor. Next, ammonia solution is added to the reaction mixture to initiate hydrolysis of TTB<sup>[36]</sup> in order to obtain a conformal and firm coating of an amorphous  $\text{TiO}_2$  layer on the surface of the C spheres (Figure 1, step a). A uniform and stable  $\text{C@TiO}_2$  core/shell structure is formed after the reaction, the formation of which is aided by the presence of many hydrophilic functional groups on the surface of the C spheres. Finally, polycrystalline  $\text{TiO}_2$  hollow spheres composed of small nanocrystals can be obtained after a simple thermal annealing treatment in air (Figure 1, step b). Importantly, this synthesis does not require delicate control of the sol–gel chemistry for the deposition of amorphous  $\text{TiO}_2$  on C spheres. In many systems, formation of a uniform shell of sol–gel-derived amorphous  $\text{TiO}_2$  on templates (for example silica spheres) has been shown to be nontrivial.<sup>[37–39]</sup>

The morphological characterizations of the  $\text{C@TiO}_2$  core/shell intermediate and crystalline  $\text{TiO}_2$  hollow spheres are shown in Figure 2. Both the field emission scanning electron microscopy (FESEM) and transmission electron microscopy (TEM) images show uniform  $\text{C@TiO}_2$  core/shell spheres prepared through the controlled hydrolysis of TTB on the surface of C spheres (Figures 2 A,B). The amorphousness of the  $\text{C@TiO}_2$  spheres is confirmed by selected-area electron diffraction (SAED) analysis (see Figure S1 in the Supporting Information). The diameter of these core/shell spheres is in the range of 600 to 800 nm and the variation of diameter is mainly because of the size distribution of the C spheres. After thermal annealing treatment, the spherical morphology is perfectly retained (Figure 2 C), and the surface of the spheres is composed of nanoparticles as shown in the magnified FESEM image (Figure 2 D). The hollow center of the annealed product is clearly shown through the TEM images (Figures 2 E,F). Unlike the  $\text{C@TiO}_2$  core/shell structure, a spherical interior with a distinct contrast difference to the

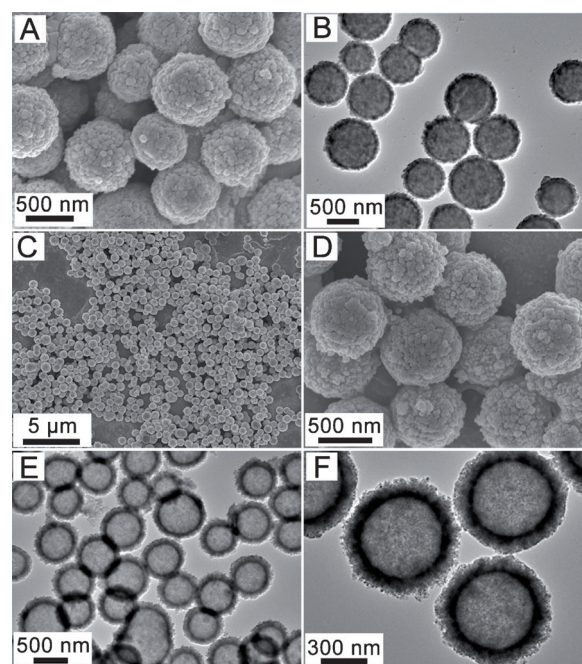


**Figure 2.** Morphological characterization of  $\text{C@TiO}_2$  and  $\text{TiO}_2$  hollow spheres: A) FESEM and B) TEM images of  $\text{C@TiO}_2$  core/shell spheres; C, D) FESEM and E, F) TEM images of crystallized  $\text{TiO}_2$  hollow spheres under different magnifications.

shell is evident in the center of the annealed spheres. The shell thickness is estimated to be about 100 nm with a relatively rough outer surface. The typical diameter of  $\text{TiO}_2$  hollow spheres decreases slightly to about 500–700 nm. This could be ascribed to a contraction effect caused by the decomposition of C spheres at elevated temperature. The phase purity of the annealed sample is examined by powder X-ray diffraction (XRD) analysis (Figure S2), where the diffraction pattern can be readily indexed to the anatase  $\text{TiO}_2$  phase (JCPDS card no. 21-1272). The broadened diffraction peaks suggest that the nanocrystals are small in size. According to the Scherrer formula, the average crystallite size is calculated to be approximately 9.1 nm.

The microstructure of  $\text{TiO}_2$  hollow spheres is further analyzed by high-resolution TEM (HRTEM), as shown in Figure 3. Lattice fringes are clearly evident from both the center (Figure 3 B) and the edge (Figure 3 C) of a randomly selected  $\text{TiO}_2$  hollow sphere shown in Figure 3 A. These lattice fringes indicate that the product is highly crystalline after thermal annealing. The interplanar distance between the lattice fringes is measured to be 0.35 nm, which can be indexed to (101) crystal planes of anatase  $\text{TiO}_2$ . Additionally, there are notable grain boundaries from the lattice fringes shown in Figures 3 B and C, which indicate that the shell of the hollow spheres is composed of small nanocrystals. The size of the nanocrystals is estimated to be approximately 10 nm, which is in good agreement with the value calculated from XRD analysis. These  $\text{TiO}_2$  hollow spheres show a relatively high Brunauer–Emmett–Teller (BET) specific surface area of  $71.2 \text{ m}^2 \text{ g}^{-1}$  ( $\text{N}_2$  adsorption-desorption isotherms are given in Figure S4). The SAED pattern of  $\text{TiO}_2$  hollow spheres

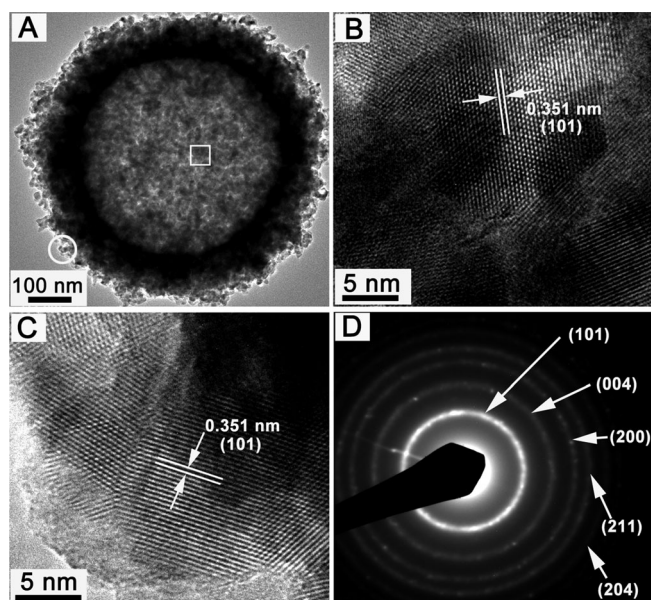


**Figure 3.** A) TEM image of an individual  $\text{TiO}_2$  hollow sphere upon which the microstructure analysis is performed; B) HRTEM image taken from the part of the hollow sphere indicated with a square in (A); C) HRTEM image taken from the part of the hollow sphere indicated with a circle in (A); D) corresponding SAED pattern.

(Figure 3D) again indicates the polycrystalline nature of the sample and each of the diffraction rings can be readily indexed to anatase  $\text{TiO}_2$ , which is consistent with the XRD results. Moreover, no visible gap can be detected between the nanocrystals, which implies that the hollow spheres have good mechanical integrity. The high robustness of these hollow spheres is further verified by sonicating the sample for 2 hours (Figure S3). From the TEM images, no notable variation in morphology or collapse of the hollow structure is evident. This excellent structural stability would be favorable for reversible lithium storage with prolonged cycle life.

To demonstrate the advantages of these robust  $\text{TiO}_2$  hollow spheres, we have evaluated their lithium storage properties as anode materials for LIBs. The cyclic voltammograms (Figure S5) exhibit the characteristic lithium insertion/de-insertion behavior for anatase  $\text{TiO}_2$ , with two redox peaks recorded at approximately 1.6 V and 2.3 V, respectively, versus  $\text{Li}^+/\text{Li}$ . Figure 4A shows representative discharge–charge voltage profiles within a cut-off voltage window of 1.0–3.0 V versus  $\text{Li}^+/\text{Li}$ . There are two notable voltage plateaus in the discharge–charge curves at approximately 1.7 V and 2.0 V versus  $\text{Li}^+/\text{Li}$ , respectively, which correspond to the lithium insertion/de-insertion process.<sup>[28]</sup> The initial discharge and charge capacities are 187.4 and 148.6  $\text{mA h g}^{-1}$ , respectively, leading to a high coulombic efficiency of 79.3%. Additionally, discharge and charge curves of the second and the hundredth cycles are almost identical, indicating that the electrochemical process is stable during the lithium insertion/de-insertion reactions. Figure 4B shows the cycling performance of  $\text{TiO}_2$  hollow spheres at a current density of 1 C (1 C = 173  $\text{mA g}^{-1}$ ). The capacity decays from 187.4 to 147.6  $\text{mA h g}^{-1}$  in the first 10 cycles and remains very stable up to 300 cycles. The long-term cycling stability of our  $\text{TiO}_2$  hollow spheres is superior to

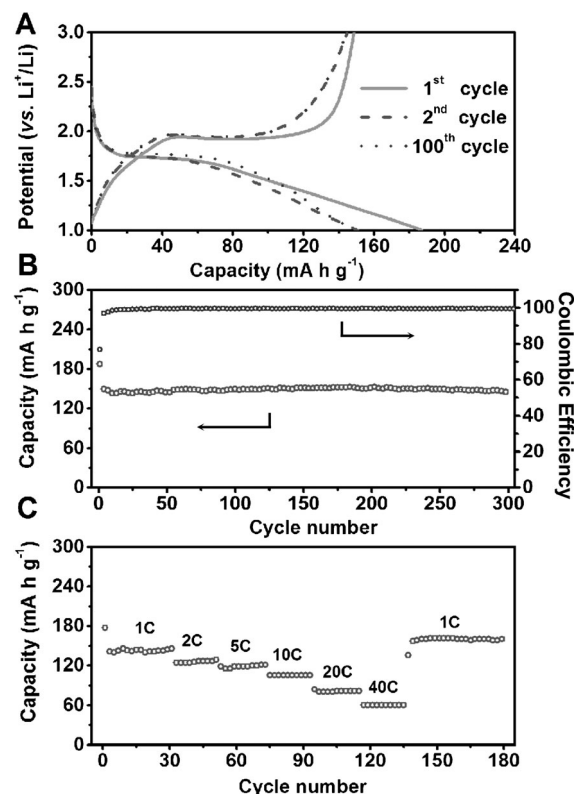


**Figure 4.** Electrochemical performance of  $\text{TiO}_2$  hollow spheres as an anode material in LIBs: A) discharge–charge voltage profiles in the voltage range of 1.0–3.0 V; B) cycling performance and corresponding Coulombic efficiency at a current rate of 1 C; C) rate performance at various current rates from 1 C to 40 C. 1 C = 173  $\text{mA g}^{-1}$ .

that of other  $\text{TiO}_2$  materials reported.<sup>[28,31,32]</sup> Moreover, these  $\text{TiO}_2$  hollow spheres exhibit excellent rate capability at discharge–charge current rates ranging from 1 to 40 C, as shown in Figure 4C. The average specific capacities are 145.2, 127.3, 120.1, 105.6, 81.4, and 60.8  $\text{mA h g}^{-1}$  at current rates of 1, 2, 5, 10, 20, and 40 C, respectively. After the high-rate discharge–charge cycling, a specific capacity of 158.2  $\text{mA h g}^{-1}$  can be restored when the current density is decreased to 1 C. Moreover, a study of the material after all cycling experiments reveals that the hollow structure is perfectly retained after cycling at 5 C for 100 cycles (Figure S6), indicating the excellent structural robustness of these  $\text{TiO}_2$  hollow spheres. These results clearly demonstrate the superior lithium storage properties of  $\text{TiO}_2$  hollow spheres in terms of long cycle life and a good rate capability for the fast charging/discharging process.

The outstanding electrochemical performance of the as-prepared  $\text{TiO}_2$  hollow spheres as anode materials for LIBs can be understood from several perspectives. First, the small size of the primary nanocrystals and the relatively thin shell offer a short diffusion distance for  $\text{Li}^+$  ions, thus promoting fast and reversible lithium insertion and extraction. Second, the robust shell structure with a sub-micrometer size effectively prevents the undesirable aggregation of conventional nanoparticles, which ensures the integrity of the electrode and improves the capacity retention upon



prolonged cycling. Third, the hollow structure with high surface area provides more active surface sites and electrolyte–electrode interface compared with solid counterparts. Additionally, the high crystallinity of TiO<sub>2</sub> hollow spheres may contribute to the electrical conductivity and crystal lattice robustness during repeated charge–discharge cycling. These features would promote the electrochemical process and lead to high specific capacity especially at high rates.

In summary, anatase TiO<sub>2</sub> hollow spheres composed of highly crystalline small nanocrystals are successfully fabricated through a simple templating approach using carbonaceous spheres as hard templates. The present method is facile and suitable for low-cost large-scale production of TiO<sub>2</sub> hollow spheres. Owing to the robust hollow structure and small primary nanoparticles, these TiO<sub>2</sub> hollow spheres exhibit exceptional lithium storage properties with ultra-stable capacity retention for over 300 cycles and excellent rate capability up to 40 C. This work is expected to be useful for the development of high-performance TiO<sub>2</sub>-based anodes for lithium-ion batteries.

Received: June 23, 2014

Revised: July 13, 2014

Published online: August 14, 2014

**Keywords:** electron microscopy · hollow spheres · lithium storage · nanostructures · titania

- [1] F. Caruso, R. A. Caruso, H. Mohwald, *Science* **1998**, 282, 1111–1114.
- [2] X. W. Lou, L. A. Archer, Z. C. Yang, *Adv. Mater.* **2008**, 20, 3987–4019.
- [3] J. Hu, M. Chen, X. S. Fang, L. W. Wu, *Chem. Soc. Rev.* **2011**, 40, 5472–5491.
- [4] X. Y. Lai, J. E. Halpert, D. Wang, *Energy Environ. Sci.* **2012**, 5, 5604–5618.
- [5] J. B. Joo, Q. Zhang, M. Dahl, I. Lee, J. Goebel, F. Zaera, Y. D. Yin, *Energy Environ. Sci.* **2012**, 5, 6321–6327.
- [6] Y. Piao, J. Kim, H. Bin Na, D. Kim, J. S. Baek, M. K. Ko, J. H. Lee, M. Shokouhimehr, T. Hyeon, *Nat. Mater.* **2008**, 7, 242–247.
- [7] Y. Zhao, L. Jiang, *Adv. Mater.* **2009**, 21, 3621–3638.
- [8] X. Wang, W. Tian, T. Zhai, C. Zhi, Y. Bando, D. Golberg, *J. Mater. Chem.* **2012**, 22, 23310–23326.
- [9] J. Wang, N. Yang, H. Tang, Z. Dong, Q. Jin, M. Yang, D. Kisailus, H. Zhao, Z. Tang, D. Wang, *Angew. Chem.* **2013**, 125, 6545–6548; *Angew. Chem. Int. Ed.* **2013**, 52, 6417–6420.
- [10] Y. J. Hong, M. Y. Son, Y. C. Kang, *Adv. Mater.* **2013**, 25, 2279–2283.
- [11] G. Q. Zhang, X. W. Lou, *Angew. Chem. Int. Ed.* **2014**, DOI: 10.1002/anie.201404604; *Angew. Chem.* **2014**, DOI: 10.1002/ange.201404604.
- [12] G. Zhang, L. Yu, H. B. Wu, H. E. Hoster, X. W. Lou, *Adv. Mater.* **2012**, 24, 4609–4613.
- [13] L. Hu, H. Zhong, X. R. Zheng, Y. M. Huang, P. Zhang, Q. W. Chen, *Sci. Rep.* **2012**, 2, 986.
- [14] Z. W. Seh, W. Y. Li, J. J. Cha, G. Y. Zheng, Y. Yang, M. T. McDowell, P. C. Hsu, Y. Cui, *Nat. Commun.* **2013**, 4, 1331.
- [15] M. H. Oh, T. Yu, S.-H. Yu, B. Lim, K.-T. Ko, M.-G. Willinger, D.-H. Seo, B. H. Kim, M. G. Cho, J.-H. Park, K. Kang, Y.-E. Sung, N. Pinna, T. Hyeon, *Science* **2013**, 340, 964–968.
- [16] Y. D. Yin, R. M. Rioux, C. K. Erdonmez, S. Hughes, G. A. Somorjai, A. P. Alivisatos, *Science* **2004**, 304, 711–714.
- [17] X. Sun, J. Liu, Y. Li, *Chem. Eur. J.* **2006**, 12, 2039–2047.
- [18] Z. H. Dong, X. Y. Lai, J. E. Halpert, N. L. Yang, L. X. Yi, J. Zhai, D. Wang, Z. Y. Tang, L. Jiang, *Adv. Mater.* **2012**, 24, 1046–1049.
- [19] X. W. Lou, C. M. Li, L. A. Archer, *Adv. Mater.* **2009**, 21, 2536–2539.
- [20] P. G. Bruce, B. Scrosati, J.-M. Tarascon, *Angew. Chem.* **2008**, 120, 2972–2989; *Angew. Chem. Int. Ed.* **2008**, 47, 2930–2946.
- [21] J. Cabana, L. Monconduit, D. Larcher, M. R. Palacin, *Adv. Mater.* **2010**, 22, E170–E192.
- [22] Y.-G. Guo, J.-S. Hu, L.-J. Wan, *Adv. Mater.* **2008**, 20, 2878–2887.
- [23] N.-S. Choi, Z. Chen, S. A. Freunberger, X. Ji, Y.-K. Sun, K. Amine, G. Yushin, L. F. Nazar, J. Cho, P. G. Bruce, *Angew. Chem.* **2012**, 124, 10134–10166; *Angew. Chem. Int. Ed.* **2012**, 51, 9994–10024.
- [24] R. Mukherjee, R. Krishnan, T.-M. Lu, N. Koratkar, *Nano Energy* **2012**, 1, 518–533.
- [25] A. S. Aricò, P. Bruce, B. Scrosati, J.-M. Tarascon, W. Schalkwijk, *Nat. Mater.* **2005**, 4, 366–377.
- [26] J. S. Chen, Y. L. Tan, C. M. Li, Y. L. Cheah, D. Y. Luan, S. Madhavi, F. Y. C. Boey, L. A. Archer, X. W. Lou, *J. Am. Chem. Soc.* **2010**, 132, 6124–6130.
- [27] X. W. Lou, L. A. Archer, *Adv. Mater.* **2008**, 20, 1853–1858.
- [28] Z. Y. Wang, X. W. Lou, *Adv. Mater.* **2012**, 24, 4124–4129.
- [29] S. T. Myung, N. Takahashi, S. Komaba, C. S. Yoon, Y. K. Sun, K. Amine, H. Yashiro, *Adv. Funct. Mater.* **2011**, 21, 3231–3241.
- [30] X. Chen, S. S. Mao, *Chem. Rev.* **2007**, 107, 2891–2959.
- [31] J. P. Wang, Y. Bai, M. Y. Wu, J. Yin, W. F. Zhang, *J. Power Sources* **2009**, 191, 614–618.
- [32] L. Xiao, M. L. Cao, D. D. Mei, Y. L. Guo, L. F. Yao, D. Y. Qu, B. H. Deng, *J. Power Sources* **2013**, 238, 197–202.
- [33] F. Gligor, S. W. de Leeuw, *Solid State Ionics* **2006**, 177, 2741–2746.
- [34] S. J. Ding, T. Q. Lin, Y. M. Wang, X. J. Lu, F. Q. Huang, *New J. Chem.* **2013**, 37, 784–789.
- [35] X. M. Sun, Y. D. Li, *Angew. Chem.* **2004**, 116, 607–611; *Angew. Chem. Int. Ed.* **2004**, 43, 597–601.
- [36] W. Li, J. P. Yang, Z. X. Wu, J. X. Wang, B. Li, S. S. Feng, Y. H. Deng, F. Zhang, D. Y. Zhao, *J. Am. Chem. Soc.* **2012**, 134, 11864–11867.
- [37] L. Yu, H. B. Wu, X. W. Lou, *Adv. Mater.* **2013**, 25, 2296–2300.
- [38] J. B. Joo, I. Lee, M. Dahl, G. D. Moon, F. Zaera, Y. Yin, *Adv. Funct. Mater.* **2013**, 23, 4246–4254.
- [39] Z. Yang, Z. Niu, Y. Lu, Z. Hu, C. C. Han, *Angew. Chem.* **2003**, 115, 1987–1989; *Angew. Chem. Int. Ed.* **2003**, 42, 1943–1945.